

Analysis of chosen IGBT faults diagnostic variables in AC/DC line-side converter

Abstract. In this paper single IGBT open-circuit faults symptoms analysis in the voltage-oriented-controlled AC/DC converter has been carried out. In accordance with the research, chosen diagnostic signals have been selected and diagnostic variables have been defined in order to evaluate transistor faults diagnostic methods. A main goal of this article was to test and confirm an effectiveness of chosen well-known diagnosis techniques for single-switch IGBT open-circuit faults in the two-level three-phase voltage inverters, in case of a reversible AC/DC line side converter, even under asymmetric power supply. Presented results have a comparative character and they have been verified by simulation model of the AC/DC converter control structure based on a measured or an estimated grid voltage.

Streszczenie. W artykule przedstawiono wybrane symptomy uszkodzeń tranzystorów IGBT, polegających na braku przewodzenia prądu, w przekształtniku energoelektronicznym AC/DC sterowanym metodą orientacji wektora prądu względem wektora mierzonego lub estymowanego napięcia sieci. Wyselekcjonowano sygnały diagnostyczne oraz zdefiniowano zmienne diagnostyczne, na podstawie których sformułowano reguły umożliwiające identyfikację uszkodzonych tranzystorów prostownika. Głównym celem pracy było zbadanie możliwości implementacji w układach przekształtnikowych AC/DC o dwukierunkowym przepływie energii znanych metod diagnostyki awarii tranzystorów dwupoziomowego falownika napięcia, również w warunkach asymetrii sieci zasilającej prostownik. Przedstawione wyniki badań mają charakter porównawczy i zostały uzyskane za pomocą symulacyjnych modeli przekształtnika AC/DC zarówno w układzie regulacji z pomiarem jak i estymacją napięć sieci zasilającej (Analiza wybranych zmiennych diagnostycznych stosowanych do wykrywania uszkodzeń tranzystorów IGBT w przekształtniku sieciowym AC/DC).

Keywords: AC/DC line-side converter, condition monitoring, open-circuit fault

Słowa kluczowe: przekształtnik sieciowy AC/DC, diagnostyka uszkodzeń, uszkodzenie tranzystora IGBT

Introduction

An utilizing of the IGBTs in AC/DC line-side converters allows an implementation of the vector control methods for the power conversion in modern electric motor drive systems, where a bidirectional energy flow is provided. These rectifiers ensure sinusoidal shape of the grid currents and fulfill the unity power factor [1]-[3]. An application cost reduction of the vector controlled AC/DC converters, which are known as PWM rectifiers, can be obtained thanks to estimation algorithms of control variables. These algorithms allow to decrease a number of sensors that are necessary to an appropriate rectifier performance. Furthermore, the reduction of operation cost of the AC/DC converter systems is possible thanks to fault diagnosis systems, which ensure a downtime reduction as well.

A vast majority of power converter faults are IGBT open-circuit failures [4], [5]. Nowadays, many transistor fault diagnostic methods have been developed. Nevertheless, most of them concern a monitoring of voltage inverters, which supply AC machines [4]-[15]. They are only few works that deal with a power switch fault diagnosis in the AC/DC rectifiers. Moreover, most of the fault diagnostic methods, that are known from a literature, are not validated in the sensorless control structures [16].

In this article single IGBT open-circuit fault symptoms analysis in the voltage-oriented-control AC/DC converter has been conducted. The aim of this paper was to confirm an effectiveness of the well-known diagnostic methods for open-switch faults in two level voltage inverter in case of the reversible AC/DC line side converter, even under asymmetric power supply. Presented results have been achieved by utilizing simulation model of the AC/DC converter control structure based on a voltage sensor or a sensorless control technique.

Description of the control method of a line-side AC/DC converter

The analyzed control structure of AC/DC converter is presented in Fig. 1. The well-known control concept based on an orientation of a line current vector i_g versus grid voltage vector e_g is used [1]-[3].

The grid voltage vector can be calculated using known converter voltage u_p and grid choke voltage u_L , using (1) [2]:

$$(1) \quad e_{gest} = u_{pest} + u_{Lest}$$

The components of the converter voltage in a stationary frame are calculated as follows (2) [2]:

$$(2) \quad u_{p\alpha est} = \frac{2}{3} U_{DC} \left(K_A - \frac{1}{2} (K_B + K_C) \right)$$

$$u_{p\beta est} = \frac{\sqrt{3}}{3} U_{DC} (K_B - K_C)$$

where: U_{DC} – capacitor voltage at the converter output, $K_{A,B,C}$ – output signals of the hysteresis controllers in suitable converter phases.

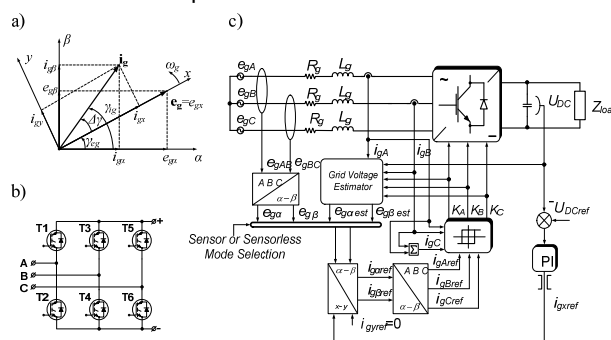


Fig.1. Control structure of AC/DC converter with grid current vector oriented versus grid voltage vector: (a) vector diagram illustrating the control idea, (b) AC/DC line-side converter scheme, (c) block diagram of the converter control structure.

The grid choke voltages are calculated using (3) [2]:

$$(3) \quad u_{L\alpha est} = -\frac{2}{3} \frac{1}{i_{g\alpha}^2 + i_{g\beta}^2} i_{g\beta} q_L$$

$$u_{L\beta est} = \frac{2}{3} \frac{1}{i_{g\alpha}^2 + i_{g\beta}^2} i_{g\alpha} q_L$$

where: $i_{g\alpha,\beta}$ – components of the grid current vector in the stationary frame, q_L – transient value of a reactive power of a choke L_g , obtained using (4) [2]:

$$(4) \quad q_L = \frac{3L_g}{\sqrt{3}} \left(\frac{di_{gA}}{dt} i_{gC} - \frac{di_{gC}}{dt} i_{gA} \right)$$

where: $i_{gA,B,C}$ – grid line currents.

Influence of IGBT faults to the AC/DC converter control system operation

The control structure of AC/DC line-side converter was tested in simulations (using *Matlab/Simulink* modeling). Below an analysis of the influence of a single IGBT open-circuit fault symptoms on state variable transients of the AC/DC converter is presented. The simulation of the respective transistor faults are modeled at the instant $t=0.3$ s during a steady-state operation of the AC/DC converter, under rectifier operation (energy taken from the grid), with resistive-inductive load Z_{load} (see Appendix 1). Presented results have a comparative character and they were achieved by utilizing simulation model of the AC/DC converter control structure based not only on voltage sensors but also on a sensorless control idea. Due to an application of a filtering capacitor (Fig. 1c) with a respectively high value and grid chokes L_g in both analyzed control structures – with measured grid voltages as well as in the sensorless solution – pulsations of the output converter voltage U_{DC} caused by a faulted IGBT are not significant (see Fig. 2). However, the converter operation with unity power factor and sinusoidal grid currents $i_{gA,B,C}$ under the single IGBT open-circuit fault is impossible, as it is shown in Fig. 3. Thus, the application of a diagnostic system for the AC/DC converter is quite reasonable, as only a fast detection of the faulted transistor can enable a fault localization and immediate repair of a faulted switch (or transistor bridge) to prevent the emergency stoppage of the industrial processes.

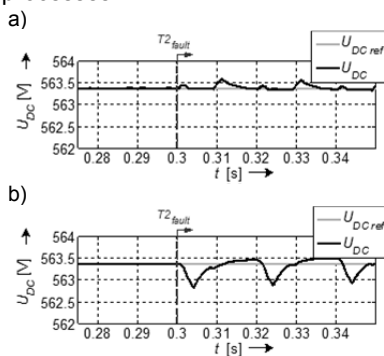


Fig.2. Transients of the DC-link voltage in the AC/DC rectifier under T2 transistor fault: (a) in the control system with the measured grid voltage, (b) in the sensorless control system.

Diagnostic methods of the power electronics converters can be classified in two types: the first ones – which use the processed current signals, and the second ones – which use the processed voltage signals. In the further part of this article, the methods used in the diagnosis of the faulted IGBT's in voltage inverters applied in electrical drives will be tested in case of the single-transistor faults in the rectifiers. In Fig. 4 transients of the *THD* (Total Harmonic Distortion) factor of the grid currents are presented, under faulted transistor in phase B of the AC/DC converter. The $THDi_g$ values for each converter phase are calculated as follows (5):

$$(5) \quad THDi_{gm} = \frac{\sqrt{\sum_{k=2}^n I_{gm k}^2}}{I_{gm 1}}$$

where: $I_{gm k}$ – RMS value of k -th harmonics of m -th grid phase, $I_{gm 1}$ – average value of a fundamental harmonics ($f_1=50$ Hz) of m -th grid phase; while $m = A, B$ or C .

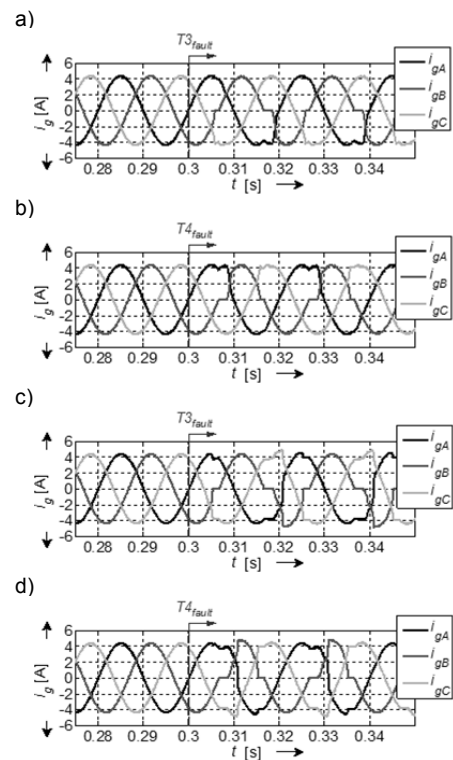


Fig.3. Transients of the grid currents of a AC/DC rectifier under T3 and T4 transistor faults: (a, b) in a control system with the measured grid voltage, (c, d) in the sensorless control system.

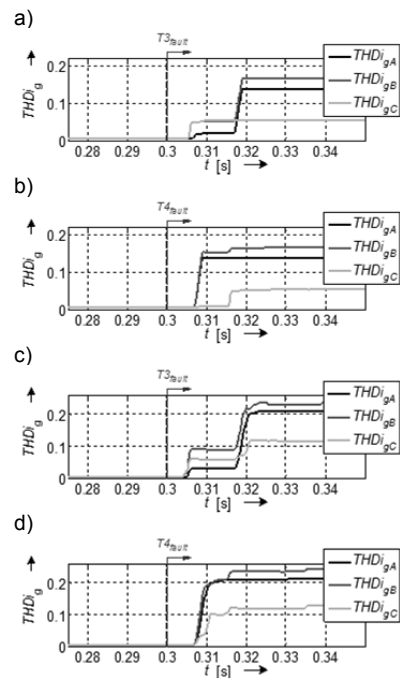


Fig. 4. Transients of the grid current *THD* coefficients under T3 and T4 transistor faults: (a, b) in the control system with the measured grid voltage, (c, d) in the sensorless control system.

Comparison of the diagnostic methods of IGBT faults in AC/DC converter

Basing on simulation results presented in previous section, it is observed a significant increase of the *THD* factor under faulted operation of the converter. In case of the transistor faults in B phase (T3 or T4), value of the $THDi_g$ factor of this current circuit is bigger than for the other ones. So, some rules, which enable the identification

(diagnosis) of the faulted converter phase, can be formulated, which are presented in the Table I. The threshold value k_{THD} can be determined using an experience obtained during simulation tests of the faulted converter behavior.

Table 1. Rules for the detection of a faulted converter phase

$THDi_{gA}$	$THDi_{gB}$	$THDi_{gC}$	Faulted transistor
$>k_{THD}$	$\in (0.25k_{THD}, 0.6k_{THD})$	$>k_{THD}$	T1 or T2
$>k_{THD}$	$>k_{THD}$	$\in (0.25k_{THD}, 0.6k_{THD})$	T3 or T4
$\in (0.25k_{THD}, 0.6k_{THD})$	$>k_{THD}$	$>k_{THD}$	T5 or T6

Moreover it was observed, that during faulty operation of the AC/DC converter controlled in a sensorless structure (with estimated grid voltage), the $THDi_g$ values for respective phases are bigger than for the control structure with measured grid voltage (see Fig. 4). In Fig. 5 transients of the average grid phase current values $\langle i_g \rangle$ under single transistor faults of phase B of the rectifier are presented, while in the next Fig. 6 transients of the control errors of the average grid phase current values $\langle \Delta i_g \rangle$, under single-transistor faults of phase C of the rectifier are illustrated.

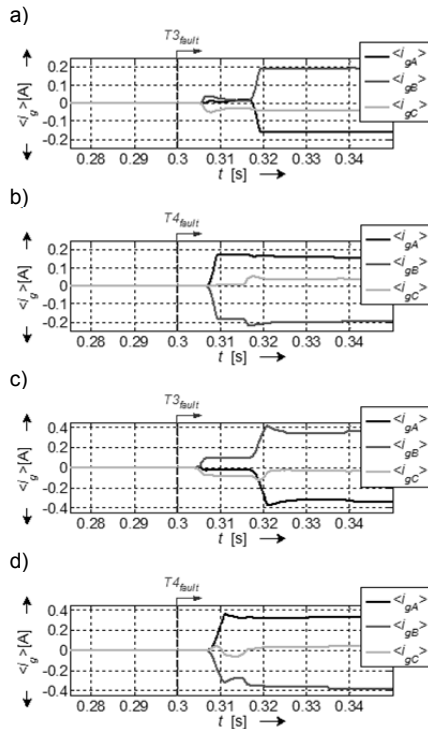


Fig.5. Transients of the average values of the grid currents under T3 and T4 transistor faults: (a, b) in the control system with the measured grid voltage, (c, d) in a sensorless control system.

The control error of the average grid phase current values is defined as follows (6):

$$(6) \quad \Delta i_{gm} = i_{gmref} - i_{gm}$$

where: i_{gmref} – the reference grid current in m -th phase, i_{gm} – measured grid current in m -th phase; while $m=A, B$ or C .

It can be seen, that for sensorless operation of the AC/DC converter, the analysis of $\langle \Delta i_g \rangle$ does not contain a diagnostic information (Fig. 6c, d) and thus cannot be considered as a diagnostic symptom. In the remain cases, under single-transistor open-circuit, as well $\langle i_g \rangle$ as $\langle \Delta i_g \rangle$ take values different than zero (Fig. 5 and Fig. 6a, b). The

set of diagnostic rules, which enable the localization of the faulted transistor are presented in Table II. The suitable thresholds k_{ig} and $k_{\Delta ig}$ are defined for the proposed diagnostic symptoms, e.g. for techniques based on the analysis $\langle i_g \rangle$ or $\langle \Delta i_g \rangle$ values. For example: if value $\langle i_{gA} \rangle$ is bigger than k_{ig} and simultaneously the value $\langle i_{gC} \rangle$ is smaller than $-k_{ig}$, then one can conclude that transistor T1 is faulted. The diagnostic rules based on the analysis of the average values of the grid currents control errors $\langle \Delta i_g \rangle$ are formulated analogically. Values k_{ig} and $k_{\Delta ig}$ can be determined using an experience achieved during simulation tests of the faulted converter behavior.

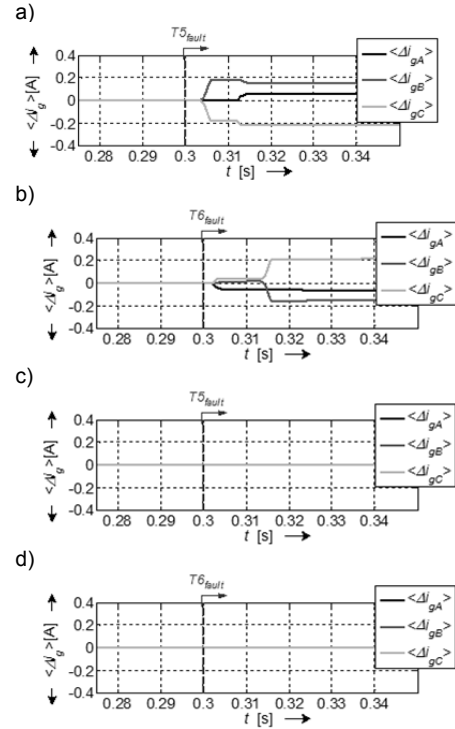


Fig.6. Transients of the average values of the grid currents control errors under T5 and T6 transistor faults: (a, b) in a control system with measured grid voltage, (c, d) in a sensorless control system.

Table 2. Rules for the detection of a faulted converter phase

$\langle i_{gA} \rangle$	$\langle i_{gB} \rangle$	$\langle i_{gC} \rangle$	$\langle \Delta i_{gA} \rangle$	$\langle \Delta i_{gB} \rangle$	$\langle \Delta i_{gC} \rangle$	Faulted transistor
$>k_{ig}$		$<-k_{ig}$	$<-k_{\Delta ig}$		$>k_{\Delta ig}$	T1
$<-k_{ig}$		$>k_{ig}$	$>k_{\Delta ig}$		$<-k_{\Delta ig}$	T2
$<-k_{ig}$	$>k_{ig}$		$>k_{\Delta ig}$	$<-k_{\Delta ig}$		T3
$>k_{ig}$	$<-k_{ig}$		$<-k_{\Delta ig}$	$>k_{\Delta ig}$		T4
	$<-k_{ig}$	$>k_{ig}$		$>k_{\Delta ig}$	$<-k_{\Delta ig}$	T5
	$>k_{ig}$	$<-k_{ig}$		$<-k_{\Delta ig}$	$>k_{\Delta ig}$	T6

One of voltage-based diagnostic methods for single-switch faults occurring in the voltage inverters has been proposed in [17]. In this article that method is tested for similar faults of AC/DC converter. In Fig. 7, the chosen transients of the average values of the estimated grid voltage $\langle e_{g est} \rangle$ under transistor faults in C phase of the rectifier, while in the next Fig. 8 – transients of the average values of the estimated grid voltage control errors $\langle \Delta e_g \rangle$ under transistor faults in A phase of the converter, in the control structure with measurement of the grid voltage. The estimated grid voltage control error is defined as follows (7):

$$(7) \quad \Delta e_{gm} = e_{gm} - e_{gmest}$$

where: e_{gm} – measured grid voltage in m -th phase, $e_{gm est}$ – estimated grid voltage in m -th phase; while $m=A, B$ or C .

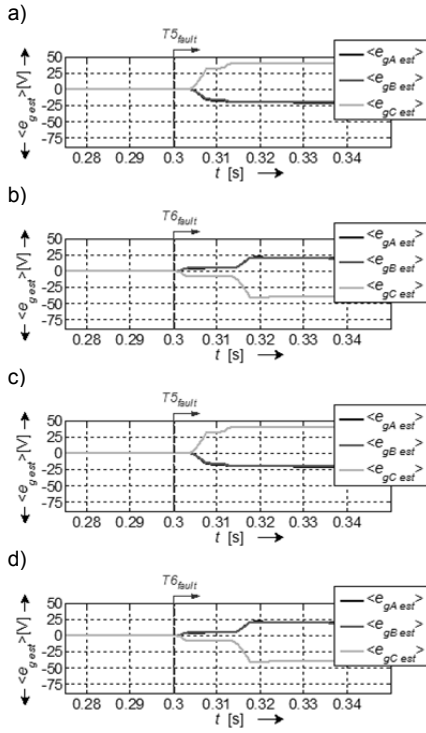


Fig.7. Transients of the average values of the estimated grid voltages under T5 and T6 transistor faults: (a, b) in the control system with the measured grid voltage, (c, d) in the sensorless control system.

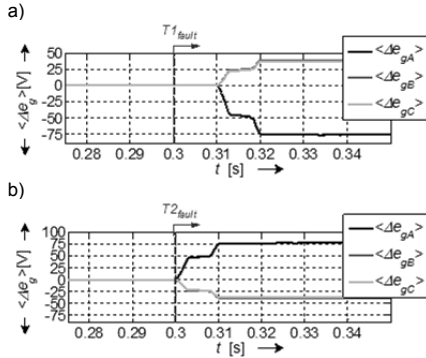


Fig. 8. Transients of the average values of the estimated grid voltage control errors under T1 (a) and T2 (b) transistor faults in the control system with the measured grid voltage.

The set of diagnostic rules, which enable the localization of the faulted transistor based on signals $\langle e_{g\ est} \rangle$ as well as $\langle \Delta e_g \rangle$, are presented in the Table 3.

Table 3. Rules for the detection of a faulted transistor

$\langle e_{gA\ est} \rangle$	$\langle e_{gB\ est} \rangle$	$\langle e_{gC\ est} \rangle$	$\langle \Delta e_{gA} \rangle$	$\langle \Delta e_{gB} \rangle$	$\langle \Delta e_{gC} \rangle$	Faulted transistor
$>k_{eg1}$	$<-k_{eg2}$	$<-k_{eg2}$	$<-k_{\Delta eg1}$	$>k_{\Delta eg2}$	$>k_{\Delta eg2}$	T1
$<-k_{eg1}$	$>k_{eg2}$	$>k_{eg2}$	$>k_{\Delta eg1}$	$<-k_{\Delta eg2}$	$<-k_{\Delta eg2}$	T2
$<-k_{eg2}$	$>k_{eg1}$	$<-k_{eg2}$	$>k_{\Delta eg2}$	$<-k_{\Delta eg1}$	$>k_{\Delta eg2}$	T3
$>k_{eg2}$	$<-k_{eg1}$	$>k_{eg2}$	$>k_{\Delta eg2}$	$>k_{\Delta eg1}$	$<-k_{\Delta eg2}$	T4
$<-k_{eg2}$	$<-k_{eg2}$	$>k_{eg1}$	$>k_{\Delta eg2}$	$>k_{\Delta eg2}$	$<-k_{\Delta eg1}$	T5
$>k_{eg2}$	$>k_{eg2}$	$<-k_{eg1}$	$<-k_{\Delta eg2}$	$<-k_{\Delta eg2}$	$>k_{\Delta eg1}$	T6

The symbols k_{eg1} , k_{eg2} and $k_{\Delta eg1}$, $k_{\Delta eg2}$ mean the diagnostic thresholds for both used signals respectively, which can be determined using simulation tests. To obtain the minimization of the faulted switch diagnostic time, the threshold values should fulfill the condition $k_{eg1} > k_{eg2}$. Similarly, for the algorithm based on the analysis of $\langle \Delta e_g \rangle$ signals, the following inequality should be fulfilled: $k_{\Delta eg1} > k_{\Delta eg2}$.

Open-switch fault diagnosis of the power converters can be also based on the information using the position γ_{ig} of current space vector in the stationary frame $\alpha\text{-}\beta$ [12], [16].

Under healthy operation of the AC/DC converter, a $\Delta\gamma$ angle between current vector and voltage vector is close to zero (see Fig. 1a). However, under single-switch fault, the grid current vector i_g stops its rotation in a characteristic part of $\alpha\text{-}\beta$ plane. Thus, monitoring the dynamics of an angle γ_{ig} , and using an information on grid currents polarization, the faulted transistor of the converter can be successfully detected and localized.

Transients of γ_{eg} or $\gamma_{eg\ est}$, γ_{ig} and $\Delta\gamma$ for the tested AC/DC converter are shown in Fig. 9, under T3 or T4 transistor faults. In this article, the diagnostic algorithm has been proposed, which can be used in the AC/DC converter with measurements of the grid voltages, basing on the information on $\Delta\gamma$ angle value (see Fig. 1a).

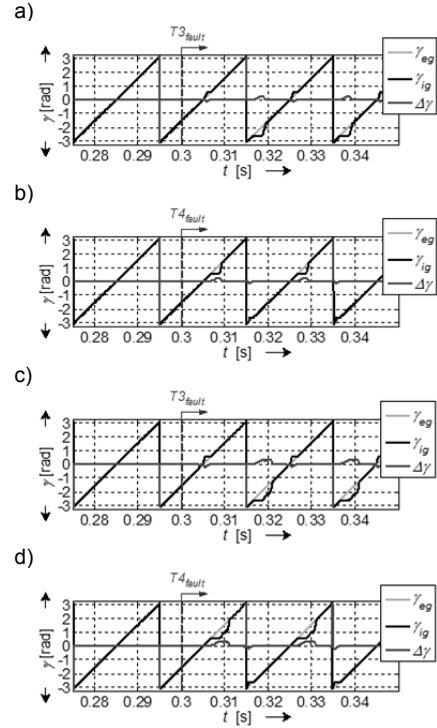


Fig.9. Transients of γ_{eg} or $\gamma_{eg\ est}$, γ_{ig} and $\Delta\gamma$ under T3 and T4 transistor faults: (a, b) in the control system with the measured grid voltage, (c, d) in the sensorless control system.

Table 4. Rules for the detection of a faulted transistor

$\gamma_{fault}[\text{rad}]$	1.57	-1.57	0.52	-2.61	2.62	-0.52
$\Delta\gamma > k_{\Delta\gamma}$	T1	T2	T4	T3	T6	T5
$\Delta\gamma < -k_{\Delta\gamma}$	T2	T1	T3	T4	T5	T6

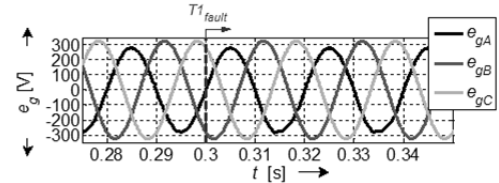


Fig.10. Transients of the asymmetric grid voltages before and shortly after the T1 fault occurrence.

The rules for the transistor fault localization are summarized in Table 4. As it was mentioned above, under faulted AC/DC converter operation, grid current vector stops its rotation in $\alpha\text{-}\beta$ plane twice, while the grid voltage always rotates with the same angular speed $\omega_{eg} = 2\pi f_{eg}$, where f_{eg} – a frequency of the grid. If $f_{eg} = \text{const.}$, so the information on $\Delta\gamma$ value and the information on the grid current vector i_g position in $\alpha\text{-}\beta$ plane, which just stopped its rotation ($\gamma = \gamma_{fault}$), enables the reliable localization of the damaged transistor

of the AC/DC converter. In the Table 4, the symbol $k_{\Delta\gamma}$ means the fault threshold, which can be determined using previous simulation test of the system.

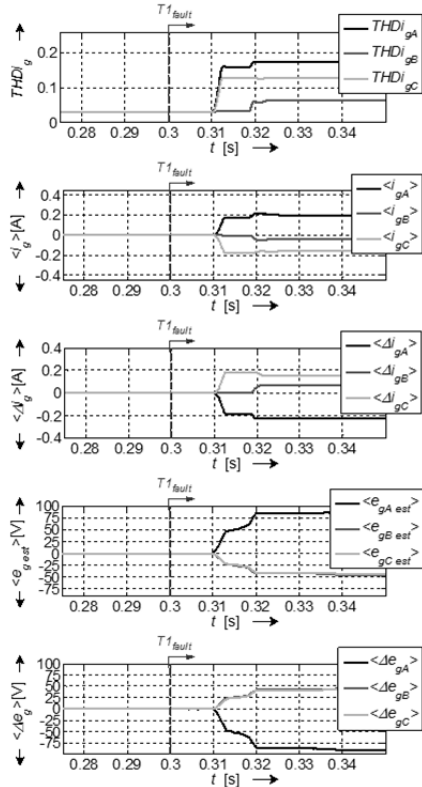


Fig. 11. Transients of the transistor fault diagnostic variables under T1 faults in the rectifier supplied by the asymmetric voltage source in the control system with the measured grid voltage.

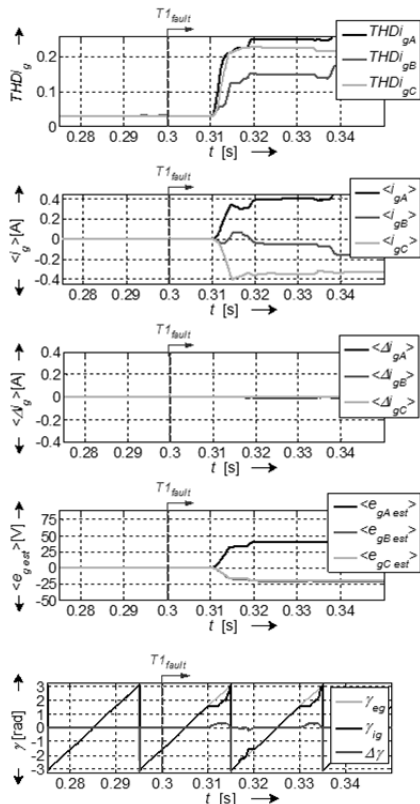


Fig.12. Transients of the transistor fault diagnostic variables under T1 faults in the rectifier supplied by the asymmetric voltage source in the sensorless control system.

From a practical point of view, it is demanded to verify an effectiveness of the transistor fault diagnostic algorithms under an asymmetric power supply condition (see Fig. 10-12). For this reason, the fault of T1 transistor in the rectifier, which is supplied by source of asymmetric voltages (see Fig. 10), was simulated.

As can be seen, a voltage amplitude in the phase A is decreased about 25V compared to other rectifier phases. In Fig. 11-12 time-domain waveforms of the transistor fault diagnostic variables in the control system with the voltage measurements (see Fig. 11) as well as for the sensorless control (see Fig. 12) structure are shown. As can be seen, the relevant observations from the previous analysis are valid for the faulted rectifier, which is fed by asymmetric voltage source.

Conclusions

In this paper the analysis of the single IGBT open-switch fault influence to the voltage-oriented-control AC/DC converter operation was presented. The control structure with measured as well as estimated grid voltage was taken into account and state variables transients of both structures under healthy and faulty converter switches in different phases were demonstrated. Basing on the diagnostic methods developed for voltage inverters supplying AC motor drives, chosen methods were adopted to the rectifiers analyzed in this paper.

In the analyzed operation conditions of the AC/DC converter, with measured grid voltages as well as in sensorless system, the output voltage pulsations caused by single-switch faults are almost negligible. However, due to the significant distortion in the grid current shape as well as difficulties in obtaining unity power factor of the system in the case of faulty transistor of the converter, some diagnostic and fault localization methods should be developed to prevent undesirable faulty brakes in the operation of industrial processes controlled using AC/DC converters.

The choice of the diagnostic method depends significantly on the applied control algorithm. As it has been shown in this paper, the methods of rectifiers transistor faults diagnosis, which are based on the analysis of the average values of grid current control errors and Clark transformation are ineffective in the sensorless system. However, they are effective in the control system with measured grid voltage. On contrary, in the sensorless control system, the methods which are based on the analysis of average values (DC component) of grid phase currents, converter current control errors or estimated grid voltages can be fully used for transistor open-circuit faults detection and localization in vector controlled AC/DC converters.

Moreover, the application of the estimation algorithm of the grid voltages enables to obtain lower cost of the whole control system by avoiding the voltage sensors as well simultaneously to increase a reliability of the system. According to the proposed voltage estimation method, the grid voltage is calculated using knowledge of the transistor control signals of the AC/DC converter. Thus, under a fault of a single transistor, the estimated grid voltage is calculated with some error, which results in bigger distortion of the converter phase currents. But yet this phenomenon enhance the effectiveness and quickness of the proposed diagnostic methods of the AC/DC converter (Fig. 4, 5).

In the future works Authors will try to verify the operation and effectiveness of the presented diagnostic methods of the line-side AC/DC converters under its operation in recuperating mode.

Appendix 1

Table 5. Data of the system

Quantity	Symbol	Value
Grid choke inductance	L_g	15mH
DC-link capacity	C	2.5mF
Load resistance	R_{load}	150 Ω
Load inductance	L_{load}	10mH
Maximal switching frequency	f_{max}	30kHz

This research work was supported by National Science Centre (Poland) under project UMO-2014/15/N/ST7/04676

Authors: Piotr Sobański, M.Sc., Teresa Orłowska-Kowalska, D.Sc., Ph.D., Prof., Wrocław University of Technology, Department of Electrical Machines, Drives and Measurements, ul. Wybrzeże Wyspiańskiego 27, 57-370 Wrocław, piotr.sobanski@pwr.edu.pl, teresa.orlowska-kowalska@pwr.edu.pl

REFERENCES

- [1] Malinowski M., Kazmierkowski M. P., Trzynadlowski A. M., A Comparative Study of Control Techniques for PWM Rectifiers in AC Adjustable Speed Drives, *IEEE Trans. on Pow. Electr.*, 18 (2003), n.6, 1390-1396
- [2] Knapczyk M., Nonlinear control strategies of AC/DC line-side converters using sliding-mode approach, Ph.D. Thesis, Wrocław University of Technology (2004)
- [3] Lee D. C., Lim D. S., AC Voltage and Current Sensorless Control of Three-Phase PWM Rectifiers, *IEEE Trans. on Pow. Electr.*, 17 (2002), n.6, 883-890
- [4] Yang S, Xiang D., Bryant A., Mawby P., Ran L., Tavner P., Condition Monitoring for Device Reliability in Power Electronic Converters: A Review, *IEEE Trans. on Power Electronics*, 25 (2010), n.11, 2734–2752
- [5] Alavi M., Wang D., Luo M., Short-Circuit Fault Diagnosis for Three-Phase Inverters Based on Voltage-Space Patterns, *IEEE Trans. on Industrial Electronics*, 61 (2014), n.5, 5558-5569
- [6] Sleszynski W., Nieznanski J., Cichowski A., Open-Transistor Fault Diagnostics in Voltage-Source Inverters by Analyzing the Load Currents, *IEEE Trans. on Industry Appl.*, 56 (2009), n.11, 4681–4688
- [7] Alavi M., Luo M., Wang D., Bai H., IGBT fault detection for three phase motor drives using neural networks, 17th Conf. on Emerging Technol. and Factory Autom., (2012), 1-8
- [8] Campos-Delgado D.U., Pecina-Sánchez J.A., Rivelino Espinoza-Trejo D., Román Arce-Santana E., Diagnosis of open-switch faults in variable speed drives by stator current analysis and pattern recognition, *IET Electric Pow. Appl.*, (2013), n.7, 509-522
- [9] An Q., Sun L., Sun L., Current Residual Vector-Based Open-Switch Fault Diagnosis of Inverters in PMSM Drive Systems, *IEEE Trans. on Pow. Electron.*, (2015), n.5, 2814-2827
- [10] Estima J.O., Marques Cardoso A.J., A New Algorithm for Real-Time Multiple Open-Circuit Fault Diagnosis in Voltage-Fed PWM Motor Drives by the Reference Current Errors, *IEEE Trans. on Ind. Electron.*, (2013), n.8, 3496-3505
- [11] Rivelino Espinoza-Trejo D., Campos-Delgado D.U., Bossio G., Bárcenas E., Hernández-Díez J.E., Lugo-Cordero L.F., Fault diagnosis scheme for open-circuit faults in field-oriented control induction motor drives, *IET Pow. Electron.*, (2013), n.5, 869-877
- [12] Orłowska-Kowalska T., Sobanski P., Simple diagnostic technique of a single IGBT open-circuit faults for a SVM-VSI vector controlled induction motor drive, *Bull. of the Pol. Acad. of Sci. Tech. Sci.*, 63 (2015), n.1, 281–288
- [13] Lu B., Sharma S.K., A literature review of IGBT fault diagnostic and protection methods for power inverters, *IEEE Trans. on Ind. Appl.*, 45 (2009), n.5, 1770–1777
- [14] Estima J.O., Freire N.M.A., Cardoso A.J.M., Recent advances in fault diagnosis by Park's vector approach, *IEEE Workshop on Electr. Mach. Des. Control and Diagn.*, (2013), 279-288
- [15] Sobanski P., Orłowska-Kowalska T., Simple transistors fault localization algorithm for voltage inverter-fed induction motor drive (in Polish), *Scientific Papers of the Institute of Electrical Machines, Drives and Measurements of the Wrocław University of Technology. Studies and Research*, 34 (2014), 76-85
- [16] Rothenhagen K., Fuchs F. W., Performance of diagnosis methods for IGBT open circuit faults in voltage source active rectifiers, *IEEE 35th Ann. Conf. of Pow. Electr. Spec.*, 6 (2004). 4348-4354
- [17] Freire N. M. A., Estima J. O., Cardoso A. J. M., A voltage-based approach for open-circuit fault diagnosis in voltage-fed SVM motor drives without extra hardware, 20th Int. Conf. on Electr. Machine, (2004), 2378-2383